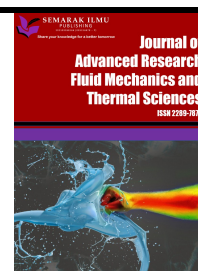




Journal of Advanced Research in Fluid Mechanics and Thermal Sciences

Journal homepage:
https://semarakilmu.com.my/journals/index.php/fluid_mechanics_thermal_sciences/index
ISSN: 2289-7879



Predicting the Influence of Densification on The Flammability Properties of Cross-Laminated Timber Using Random Forest Model

Charles Michael Albert¹, Liew Kang Chiang^{1,*}

¹ Faculty of Tropical Forestry, Universiti Malaysia Sabah, Jalan UMS, 88400 Kota Kinabalu, Sabah, Malaysia

ARTICLE INFO

Article history:

Received 2 July 2025

Received in revised form 4 November 2025

Accepted 23 November 2025

Available online 8 December 2025

Keywords:

densification, cone calorimetry, fast-growing timber, machine learning, random forest

ABSTRACT

Timber, a popular construction material, has limited application due to its vulnerability to fire. Hence, the flammability behaviour of timber is continuously studied to enhance its fire resistance. This study introduces a short-duration densification process that compresses low-density timber, enhancing its physicomaterial and flammability properties and making it suitable for heavy-duty applications. The objective of this study is to assess the effect of compression ratios on the heat release rate (HRR) and total smoke production (TSP) of the cross-laminated timber (CLT) manufactured from the laminas of *Paraserianthes falcataria*, a low-density, fast-growing timber species. The laminas were compressed at varying compression ratios (0% (control), 40%, 50%, and 60%), processed into CLT panels, and subjected to cone calorimeter test. The findings indicated that increasing compression ratios significantly enhanced density, whereas compressing the laminas at 60% resulted in a density improvement of up to 142.68%. Cone calorimeter tests revealed that incremental 10% increases in compression ratios improved flammability properties, with 60% compression ratio significantly reducing HRR and TSP. Furthermore, this study developed predictive models using random forest approach to estimate the HRR and TSP of CLT manufactured from laminas compression at varying compression ratios. By utilizing advanced regression approaches, these models provide valuable insights into the heat spread and smoke generation behaviour of CLT, potentially improving the accuracy of predictions for essential fire safety parameters.

1. Introduction

Timber is a widely recognized and valuable construction material due to its sustainability, renewability, and excellent mechanical properties [1,2]. Besides that, this material outperforms conventional materials (e.g., steel and concrete) in terms of flexibility and cost-effectiveness [2,3]. Engineered wood products, such as cross-laminated timber (CLT), are gaining popularity for their structural integrity and sustainability [4].

* Corresponding author.

E-mail address: liewkc@ums.edu.my

<https://doi.org/10.37934/arfmts.136.1.1225>

However, timber faces limitations, particularly in terms of flammability and fire safety [1]. For instance, multi-storey timber constructions face significant challenges due to the flammability of timber and its low thermal inertia [5,6]. Therefore, it is essential to thoroughly investigate and analyze the fire behaviour of loaded cross-laminated timber panels to guarantee the safety of timber structures, as suggested by various studies [1,2,4,6]. Although timber can be processed into valuable construction materials such as glued laminated timber and cross-laminated timber, the issue of its flammability continues to exist [1].

Various technologies and treatments have been used to improve the fire resistance of timber. For example, a practical approach applied by Xu *et al.*, [5] involved filling the void between timber boards with mineral wool, which provided insulation and avoided direct fire outbreaks on the unexposed side. Additionally, intumescent paints have been identified as a method to delay the start of charring, thereby increasing the fire resistance of timber structures [1,7]. Furthermore, the steel-timber composite structure, which is a combination of cold-formed steel and cross-laminated timber, has also been examined and suggested as an approach to enhance fire resistance in construction [8]. Laboratory-scale fire tests, such as the cone calorimeter, can assist researchers in efficiently analyzing and optimizing fire-resistant composite materials [5,6,8–11]. The cone calorimeter is a standardized test instrument widely used to measure the flammability properties of materials, such as heat release rate, total heat release, mass loss, time-to-ignition, smoke density, and gas concentrations [6,7,10]. Researchers have used cone calorimeter tests to assess the impact of fire retardants on wood composites such as melamine, zinc borate, and ammonium polyphosphate, to enhance fire resistance [7,12,13]. Moreover, this test has been vital in studying the fire resistance of wood coatings containing nitrogen and phosphorus-containing compounds, providing valuable data on parameters like limiting oxygen index and pyrolysis behaviour, and contributing to developing fire-safe products [14]. Besides that, another study by Hasburgh and Zelinka [15] stated that this test has been instrumental in evaluating the flammability of acetylated wood under different burning conditions, offering insights into char formation, pyrolysis behaviour, and acetic acid emissions during combustion.

Densification is a treatment that can enhance the physicomechanical properties of timber by compressing its porous structure, typically under heat and pressure [3,16]. Various studies have shown that engineered wood products, such as CLT, manufactured from densified timber, exhibited improved density, dimensional stability, and mechanical strength (e.g., hardness, flexural strength, and compression) compared to CLT made from untreated timber [3,17]. Besides that, densification also enhances the flammability properties of timber, i.e., during densification, wood is subjected to heat and pressure, resulting in increased density and the development of a more compact structure, which inhibits oxygen diffusion inside the wood capillaries [3,16,18,19]. For instance, a study by Gan *et al.*, [16] reported that densification created a functionalized surface layer on timber that acts as a barrier to oxygen infiltration, which delayed pyrolysis reactions and enhanced char formation. Despite having excellent physicomechanical properties, comprehensive studies on the flammability properties of cross-laminated timber (CLT), especially when manufactured from densified timber, remain limited. Random forest (RF) model is an ensemble learning method primarily used for classification and regression tasks, where the algorithm develops multiple decision trees during training and merge their outputs to improve predictive accuracy and resist overfitting [20,21]. RF is capable to handle large datasets, both in categorical and numerical data, and performs well even with unbalanced datasets to provide high accuracy predictions [21]. Moreover, this data-driven modeling approach is often applied in bioinformatics, finance, and ecology due to its ability to capture complex non-linear relationships [20]. Despite that, machine learning algorithm has not been

applied to predict wood's characteristics (e.g., flammability), due to reliance on the existing mechanistic models.

While densification is known to improve density, the specific relationship between incremental increases in compression ratios in densification and the key flammability parameters has not been clearly assessed. Therefore, this study investigates the influence of varying compression ratios on the flammability properties of cross-laminated timber (CLT) manufactured from densified timber. In this research, laminas of *Paraserianthes falcataria*, a fast-growing, low-density timber species, were subjected to short-duration densification at varying compression ratios, ranging from 40-60%. Key flammability parameters, such as heat release rate and total smoke release, were assessed using the cone calorimeter test. Moreover, a detailed analysis was carried out to develop predictive models that provide reliable estimations of these properties. This research aims to fill the existing knowledge gap with comprehensive empirical data, enabling effective prediction of densified CLT behaviour in fire scenarios.

2. Materials and Methods

2.1 Material Preparation

The kiln-dried laminas of *Paraserianthes falcataria* (equilibrium moisture content: 12%) were visually graded to select laminas with minimal defects, e.g., pinholes, watermarks, and cracks. The selected laminas were cut into dimensions of 300 mm (length) x 50 mm (width) x 20 mm (thickness) and conditioned (relative humidity: 65%; room temperature: 25°C) at the Faculty of Tropical Forestry, Universiti Malaysia Sabah.

2.2 Densification Process

A short-duration densification process, as shown in Figure 1, was carried out, where it involved the main stages of pressing, venting, and cooling. The densification process began with a 3-minute pressing stage, followed by a 1-minute and 40-second venting stage to relieve internal stresses, and facilitate moisture release from the laminas. Subsequently, the laminas underwent a second cycle of pressing and venting. The final stage involved pressing the laminas with heat for 1 minute, followed by a cooling phase at temperatures below 80°C for 5 minutes. The densified laminas were then conditioned (relative humidity: 65%; room temperature: 25°C) for seven days to achieve a stable set-recovery rate.

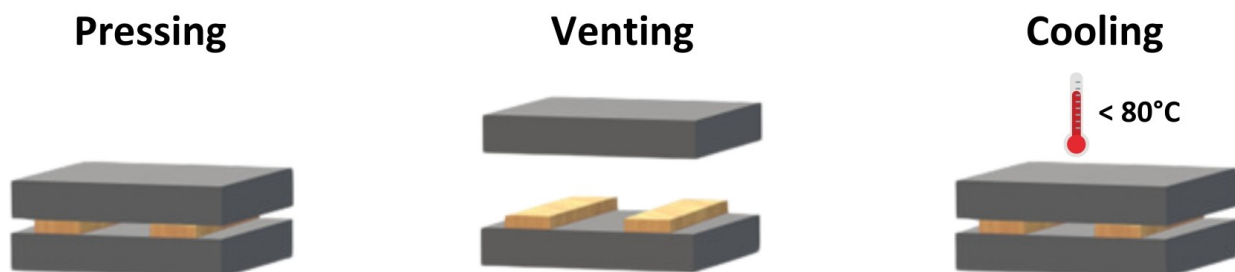


Fig. 1. Schematic visualization of the main stages during the short-duration densification process

Three compression ratios (CR) were applied to achieve the targeted thickness, as displayed in Figure 2. In the context of densification, CR refers to the degree to which the lamina is compressed during the densification process [3]. The CR was measured using Eq. (1), where CR is the compression ratio (%), t_i is the initial thickness (mm), and t_f is the targeted thickness (mm).

$$CR = \frac{t_i - t_f}{t_i} \times 100 \quad (1)$$

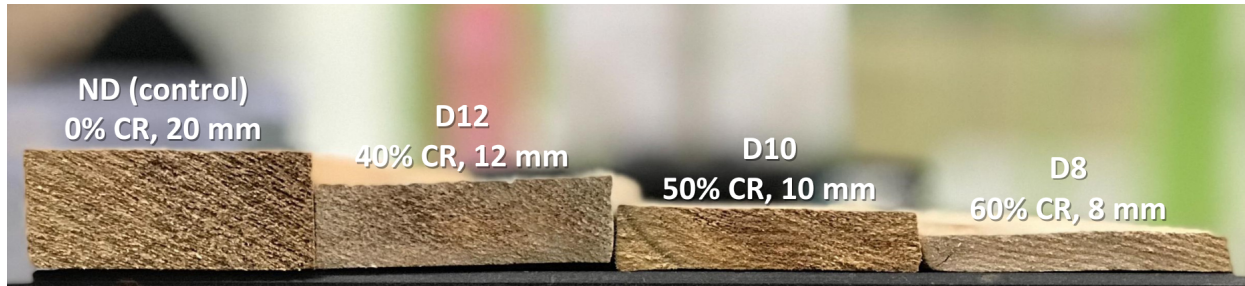


Fig. 2. The laminas of *Paraserianthes falcataria* densified at varying compression ratios

2.3 Cross-Laminated Timber Manufacturing

The edges and surfaces of the laminas were planed using a planer machine to achieve uniform width of 50 mm, because the laminas increase in width after densified. After that, the laminas were edge- and surface-glued together using polyvinyl acetate (PVAc), with glue spread of 400 g/m², and clamped for 24 hours for curing to make three-layers cross-laminated timber panels with dimensions of 300 mm (length) x 300 mm (width) x 60/46/30/24 mm (thickness).

2.4 Density Measurement

The density of the densified laminas and CLT was measured using gravimetric method, as specified in ASTM D2395 [22]. Three test pieces with dimensions of 300 mm (length) x 300 mm (width) were prepared from the laminas and CLT of each compression ratio.

2.5 Flammability Test

Three CLT test pieces from each compression ratio were cut to 100 mm (length) x 100 mm (width) and subjected to a cone calorimeter test, as illustrated in Figure 3, at the Science and Technology Research Institute for Defense (STRIDE), Selangor. The test was conducted according to ISO 5660, whereby heat flux of 50 kW/m² was applied to all test pieces, while pre-test conditions such as ambient temperature, ambient pressure, and ambient relative humidity were set to 25°C, 100.6 kPa, and 50%, respectively [23].

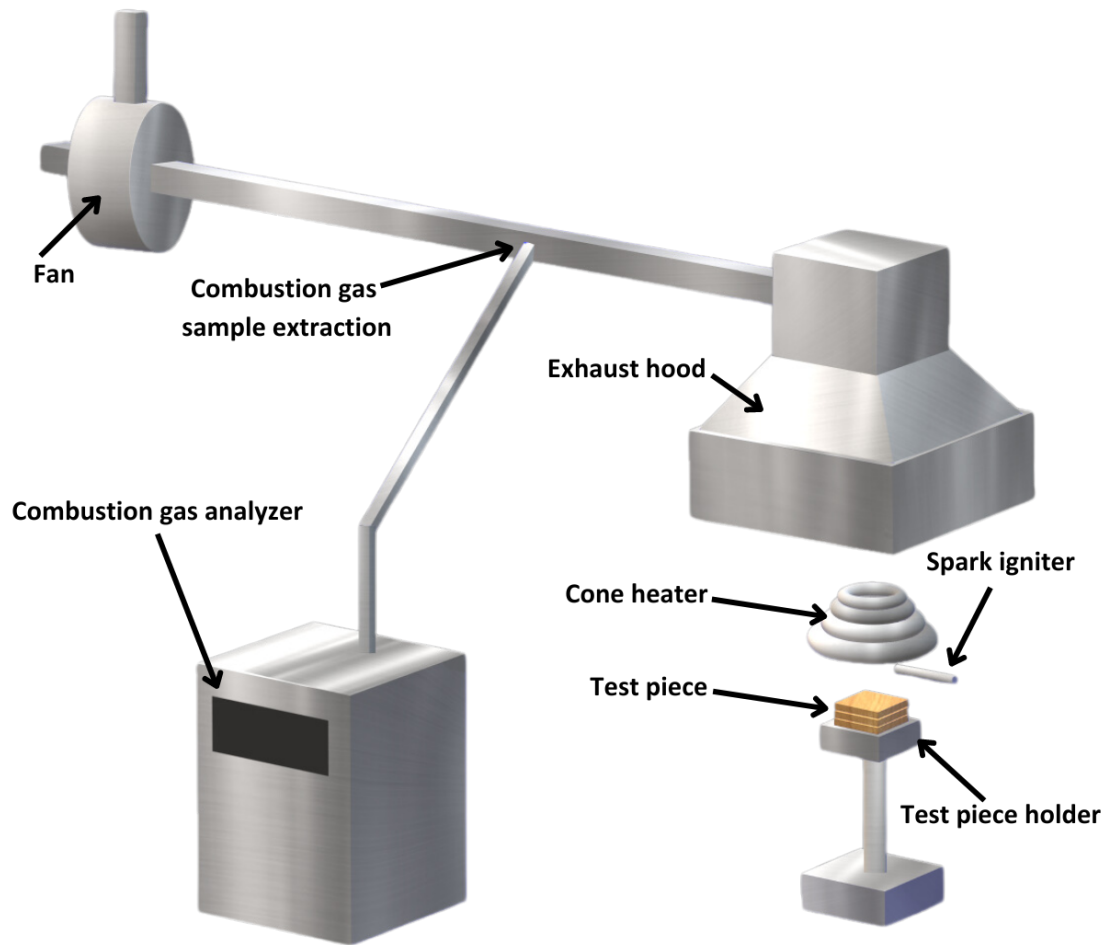


Fig. 3. Schematic diagram of the cone calorimeter setup

2.6 Statistical Analysis and Random Forest Modeling

One-Way ANOVA with a post-hoc LSD test ($p \leq 0.05$) was performed using R (Version 4.4.1) to assess the multiple comparisons between different compression ratios from the data of density measurement and cone calorimeter test. As for the model development, random forest approach was performed in R (Version 4.4.1), using the “randomForest” package, to predict the heat release rate (HRR) and total smoke production (TSP) of the CLTs manufactured from the densified laminas. Random forest (RF) is a non-parametric, versatile, and robust ensemble learning approach that can be used to construct models for regression and classification studies [20,21,24]. This approach was chosen due to its capability to handle complex interactions between variables and effectiveness in minimizing overfitting [20,21]. The model development is visualized in Figure 4.

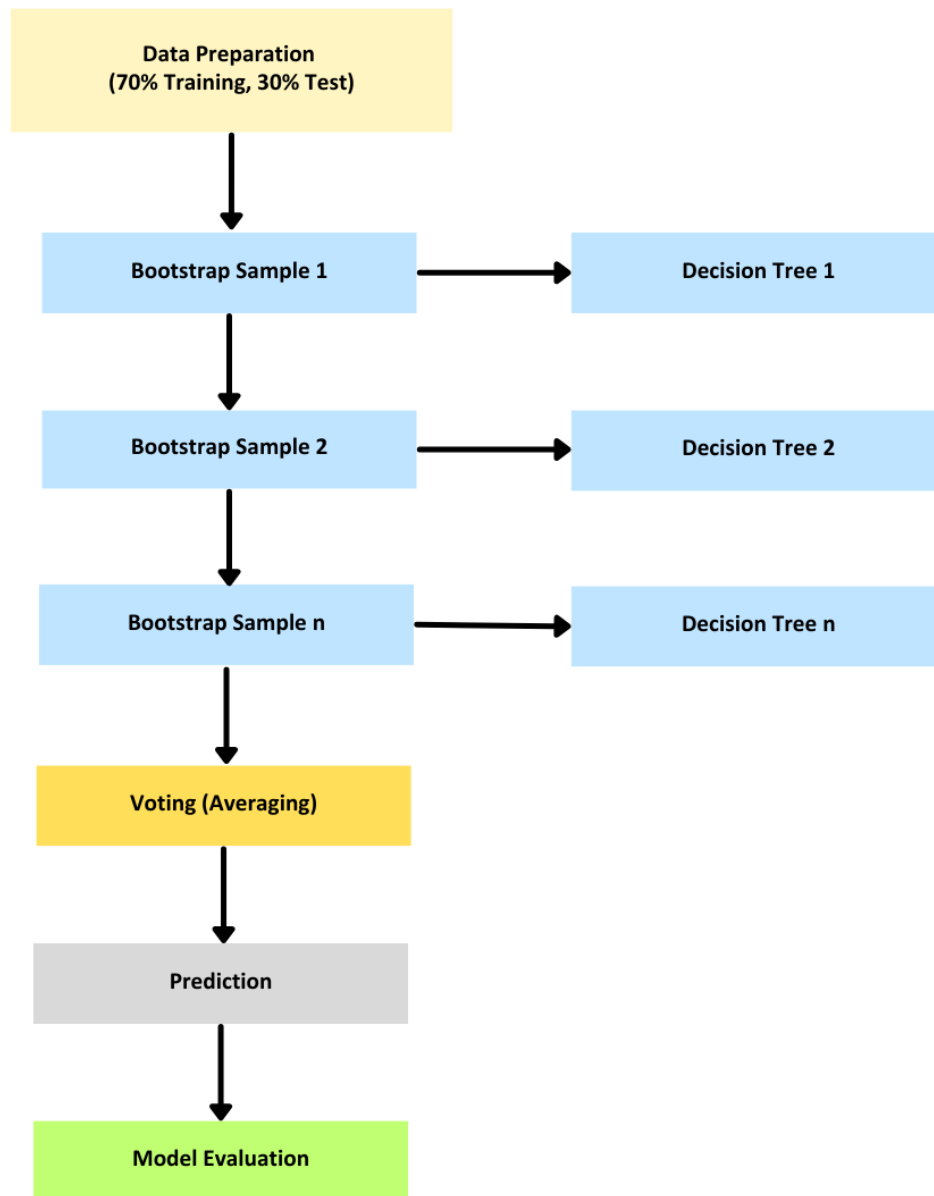


Fig. 4. Visualization of random forest model development and evaluation

The predictors for HRR included compression ratio, mass loss rate (MLR), and density. For TSP, the predictors were compression ratio, oxygen production (O2P), and carbon dioxide production (CO2P). The dataset for HRR and TSP, along with the predictor variables, was split into training and test sets, where 70% of the data was used for training the models and the remaining 30% was reserved for testing. Multiple bootstrap samples were drawn from the training data, which involved randomly sampling the data with replacement to create multiple subsets. For each bootstrap sample, a decision tree was built by repeatedly splitting the data based on the predictor variables, with each split selected to minimize the mean squared error. Subsequently, the predictions from all the decision trees were aggregated by averaging the predictions from all the trees. The models were then evaluated using several metrics, such as R-squared (R^2), Root Mean Squared Error (RMSE), Mean Absolute Error (MAE), and Cross-Validation Error (CV Error). R^2 values reflect the proportion of variance in the dependent variable that is explained by the model, where higher R^2 values indicate a better fit. The R^2 is calculated by referring to Eq. (2).

$$R^2 = 1 - \frac{\sum_{i=1}^n (y_i - \hat{y}_i)^2}{\sum_{i=1}^n (y_i - \bar{y})^2} \quad (2)$$

where y_i is the actual value, \hat{y}_i is the predicted value, \bar{y} is the mean of actual values, and n is the number of data points. RMSE, the values indicate the average deviation of the predicted values from the actual values, where lower RMSE values suggest better model performance. RMSE is computed using Eq. (3).

$$RMSE = \sqrt{\frac{1}{n} \sum_{i=1}^n (y_i - \hat{y}_i)^2} \quad (3)$$

where y_i is the actual value, \hat{y}_i is the predicted value, and n is the number of data points. Moreover, MAE values represent the average absolute error between the predicted and actual dependent variable values, whereby lower MAE values are indicative of better model performance. MAE is measured by using Eq. (4).

$$MAE = \frac{1}{n} \sum_{i=1}^n |y_i - \hat{y}_i| \quad (4)$$

where y_i is the actual value, \hat{y}_i is the predicted value, and n is the number of data points. CV Error values show the average RMSE obtained from cross-validation, whereby lower CV error values indicate better model performance and generalizability. CV error is computed using Eq. (5), where k is the number of folds, E_i is the error for each fold.

$$CV\ Error = \frac{1}{k} \sum_{i=1}^k E_i \quad (5)$$

3. Results and Discussion

3.1 Density

The results indicated that short-duration densification could effectively enhance the density of laminas, achieving a notable increase of up to 142.68%. Table 1 shows the final density of the laminas and CLT, where D8 obtained the highest density, followed by D10, D12, and the control. Moreover, there are significant differences between all the compression ratios, indicating that applying a higher compression ratio resulted in higher density. These outcomes suggest a notable improvement in mechanical properties, which are fundamental criteria for structural applications [2,17]. Previous studies on densification have reported that densified wood exhibits better flexural strength and hardness than untreated wood, attributable to the compacted structures formed during the densification process [25–28]. The densification process reduces the void spaces and creates a more uniform and compact wood structure, which significantly contributes to these improvements in mechanical strength, making densified wood a viable and competitive material for various structural and industrial applications [3,16,27].

Table 1

The targeted and actual compression ratios, and final density of densified lamina and CLT

Coding	Compression ratio (%)		Density (kg/m ³)	
	Target	Actual	Lamina	CLT
ND (Control)	0	0	297.36 _a ± 51.24	340.17 _a ± 14.35
D12	40	39.64	452.74 _b ± 83.58	441.33 _b ± 47.97
D10	50	50.48	571.33 _c ± 11.09	536.61 _c ± 16.01
D8	60	59.69	721.83 _d ± 60.82	631.09 _d ± 9.89

* The mean values of the density are displayed with subscripts a, b, c, and d to denote significant differences among different compression ratios, followed by the standard deviation values.

The slight differences between the targeted and actual compression ratios displayed in Table 1 might be influenced by factors such as moisture content, initial density, temperature and pressure during the densification process, and grain direction [18,29,30]. Higher moisture content can enhance the compressibility of the wood due to the high plasticization of its cellular structure [30]. Nevertheless, acquiring excessive moisture content would result in uneven moisture within the wood, which also might cause the densified wood to have an irregular shape and moisture pockets [26]. Moreover, the initial density of the wood also influences the final compression ratios, where low-density woods are easier to compress, often resulting in greater density increases [30]. High-density woods, on the other hand, might require higher pressure and precise control during the densification process to achieve the desired compression ratios due to their compacted structures [30].

The temperature and pressure applied during the densification process also influence the degree of compression, whereby elevated temperatures can soften the lignin, making the wood more flexible, while optimal pressure ensures uniform densification and avoids damage due to excessive mechanical pressure [3,25,27,30]. Various studies on the influence of different temperatures on the densification degree stated that elevated temperatures within 100-180°C aid the densification, resulting in woods with good dimensional stability and density, while applying 200°C did not significantly influence the plasticization rate [31–34]. Additionally, different temperatures were applied based on the wood species due to their distinct anatomical structures [31,33]. Low-density wood might need lower temperatures to promote plasticization, while high-density wood might require higher temperatures [34]. However, applying high temperatures can result in higher thermal degradation rates [30–32]. Furthermore, grain orientation affects the degree of compression [29]. Wood can be densified in different directions: radial, tangential, and longitudinal [30]. When wood is compressed radially, the lumens collapse more uniformly, leading to a consistent increase in density [35]. On the other hand, tangential and longitudinal compressions encounter more resistance due to the alignment of fibers and vessels, which can result in uneven compression and localized failures [29,35].

3.2 Flammability

Table 2 shows the statistical outputs from the cone calorimeter test, where D8 obtained the lowest heat release rate (HRR) value of 53.98 kW/m², while ND had the highest value (80.58 kW/m²). As for the total smoke production (TSP), D8 had the lowest value of 0.16 m², while ND had the highest value (3.98 m²). For these two properties, D8 was statistically significant from other groups, indicating that applying 60% compression ratio would result in a notable improvement in fire resistance. On the other hand, D12 exhibited a higher oxygen production rate (O2P) than other groups. Despite that,

there is no notable difference between the compression ratios for the mass loss rate (MLR) and carbon dioxide production (CO₂P).

Table 2

Descriptive statistics and multiple comparison for flammability properties of CLT

Coding	Heat release rate (kW/m ²)	Total smoke production (m ²)	Mass loss rate (g/s)	Oxygen production (g/s)	Carbon dioxide production (g/s)
ND (Control)	80.58 _a ± 16.77	3.98 _a ± 2.00	0.05 _a ± 0.02	20.92 _a ± 0.02	0.22 _a ± 0.02
D12	68.56 _b ± 12.58	3.07 _b ± 1.52	0.06 _b ± 0.03	20.93 _b ± 0.03	0.19 _a ± 0.03
D10	59.99 _c ± 11.26	1.64 _c ± 1.14	0.04 _a ± 0.02	20.74 _c ± 0.02	0.19 _a ± 0.03
D8	53.98 _d ± 7.91	0.16 _d ± 0.02	0.04 _a ± 0.02	20.91 _d ± 0.02	0.18 _a ± 0.03

* The mean values of the density are displayed with subscripts a, b, c, and d to denote significant differences among different compression ratios, followed by the standard deviation values.

Table 3

Model metrics for random forest approach on predicting the flammability properties of CLT

Flammability Properties	Coding	R ²	RMSE	MAE	CV Error
Heat Release Rate	ND (Control)	0.983	2.601	1.427	0.9123
	D12	0.967	2.362	1.110	0.9671
	D10	0.992	1.152	0.737	0.6801
	D8	0.944	2.050	0.920	0.5670
Total Smoke Production	ND (Control)	0.999	0.024	0.007	0.0065
	D12	0.999	0.013	0.004	0.0043
	D10	0.999	0.007	0.003	0.0040
	D8	0.982	0.011	0.002	0.0010

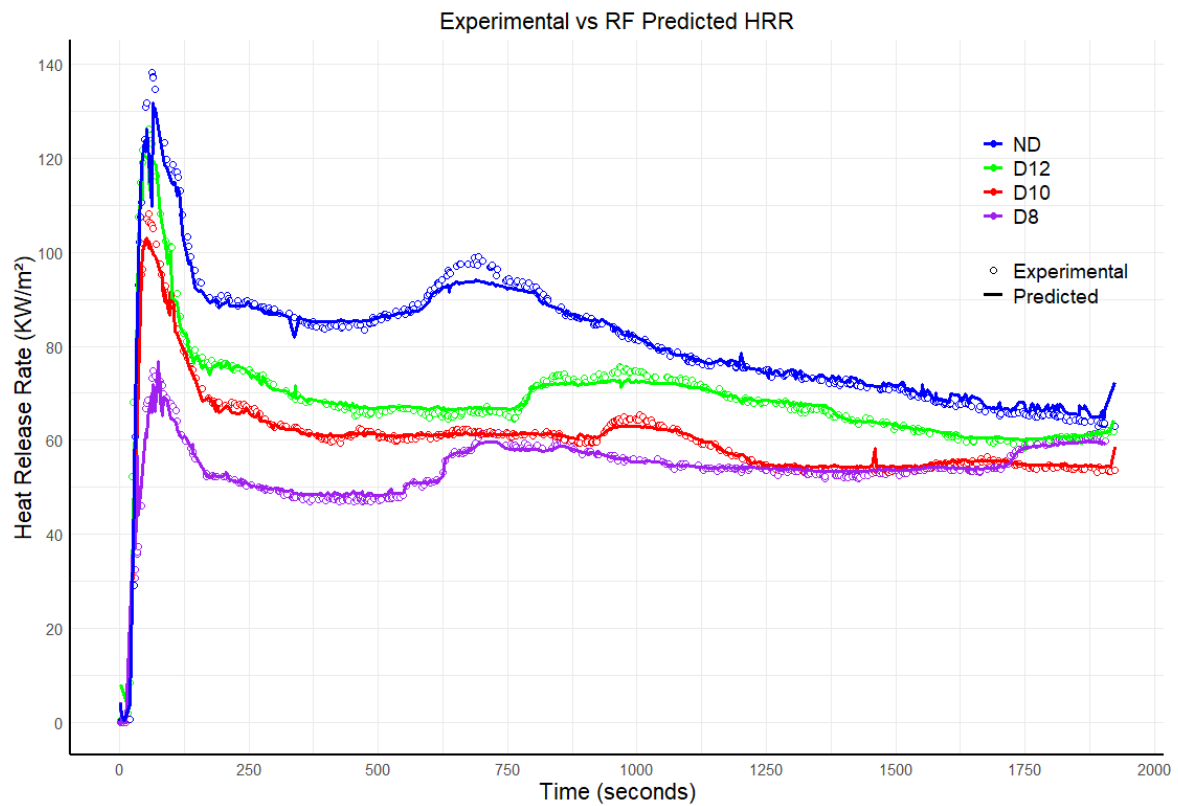


Fig. 5. The experimental and predicted heat release rate dynamics of CLT over time

The HRR values of the CLT from all compression ratios, as illustrated in Figure 5, initially increased sharply within the first 250 seconds, peaking between 100 and 140 kW/m². During this early phase, ND reached the highest peak at about 140 kW/m², indicating the lowest ignition time. During the early decline phase (250-750 seconds), HRR values reduced for all groups, with D8 maintaining the lowest average HRR at around 51 kW/m², followed by D10 at 62 kW/m², D12 at 67 kW/m², and ND at 89 kW/m². In the mid-stage (750-1250 seconds), D8 continued to show the most excellent fire resistance, with an average HRR of 56 kW/m². D10 and D12 had average HRR values of 61 kW/m² and 72 kW/m², respectively, while ND had the highest at 82 kW/m². Furthermore, D8 maintained the lowest HRR at 55 kW/m², with D10 at 54 kW/m², D12 at 62 kW/m², and ND at 69 kW/m², during the late stage (1250-1923 seconds). In summary, D8 had the lowest HRR throughout the testing period, indicating slower fire growth, which can limit fire spread and intensity. The model metrics for HRR in Table 3 indicate that using compression ratio, density, and mass loss rate as predictors yielded accurate predictions. D10 achieved the highest R² value of 0.992 and the lowest RMSE of 1.152, reflecting the most accurate predictions. ND (Control) had a lower R² of 0.983 and the highest RMSE of 2.601. D8 exhibited the lowest CV error at 0.5670, indicating the most stable model, while D12 had the highest CV error of 0.9671, suggesting less stability.

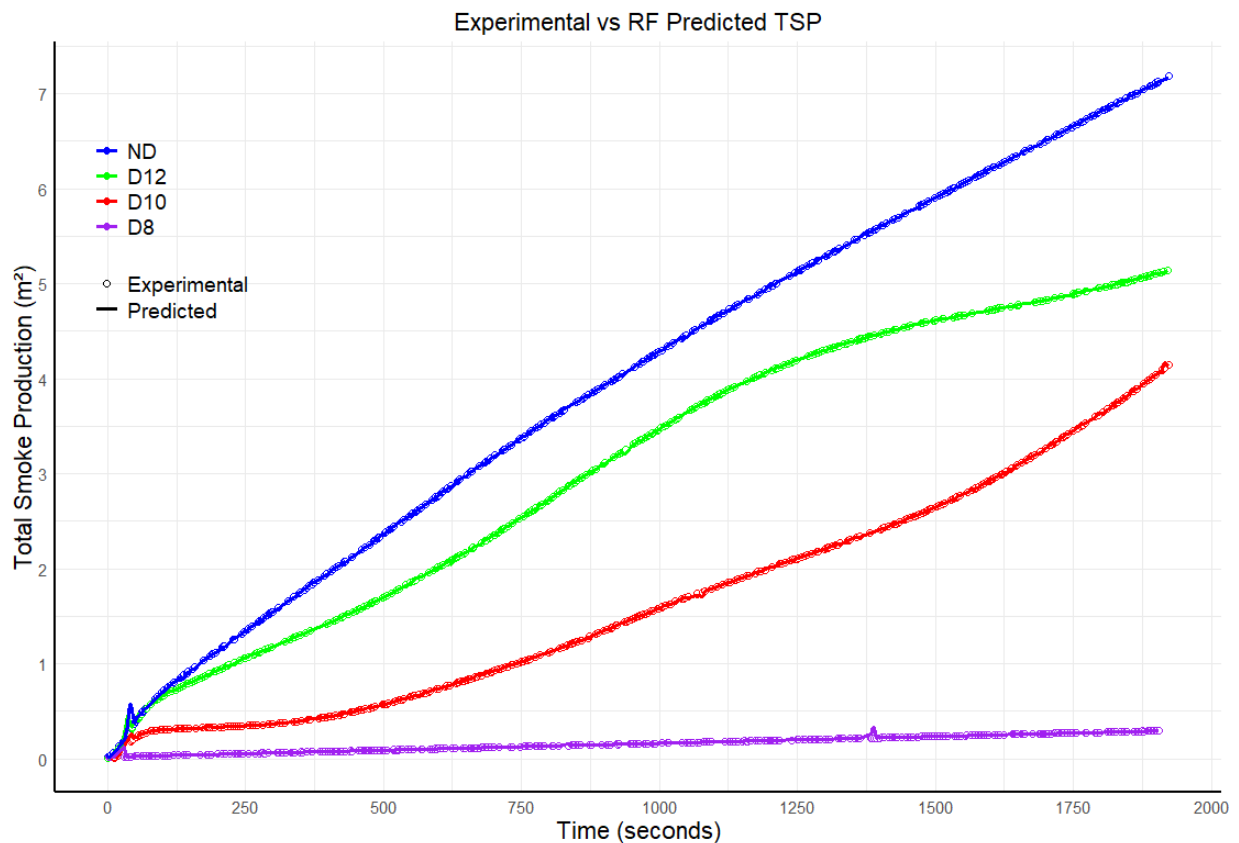


Fig. 6. The experimental and predicted total smoke production of CLT over time

The experimental result in Figure 6 shows that TSP values of all compression ratios increased during the initial stage (0-250 seconds), where ND had the highest TSP at about 0.003 m²/m², while D12 and D10 had lower TSP values than ND but higher than D8. D8 began with a TSP of 0.000 m²/m² and started to increase around the 10-second mark, indicating better initial performance in reducing smoke. During the growth stage (250-750 seconds), TSP values continued to rise, where D8 maintaining the lowest TSP, starting to show values around 0.02 m²/m², followed by D12 at

approximately $0.01 \text{ m}^2/\text{m}^2$, D10 ($0.003 \text{ m}^2/\text{m}^2$), and ND ($0.026 \text{ m}^2/\text{m}^2$). In the mid-stage (750-1250 seconds), D8 showed slightly higher values but remained the lowest among the compression ratios, while D12 and D10 showed higher values of around $0.013 \text{ m}^2/\text{m}^2$ and $0.003 \text{ m}^2/\text{m}^2$, respectively, with ND the highest at approximately $0.026 \text{ m}^2/\text{m}^2$. Moreover, D8 continued to have the lowest TSP, maintaining a value around $0.02 \text{ m}^2/\text{m}^2$, with D10 at approximately $0.003 \text{ m}^2/\text{m}^2$, D12 at around $0.013 \text{ m}^2/\text{m}^2$, and ND at approximately $0.026 \text{ m}^2/\text{m}^2$ during the late stage (1250-1923 seconds). Overall, D8 consistently had the lowest TSP values throughout the stages, indicating better smoke reduction, improving visibility during a fire scenario, and reducing the exposure to harmful gases that can cause health hazards (e.g., respiratory issues). Furthermore, the implementation of random forest modeling to estimate the TSP of CLT provides reliable and accurate predictions, as demonstrated in Table 3. D10 had the lowest RMSE of 0.007 and an R^2 of 0.999, explaining 99% of the variance. D12 also performed well with similar metrics, while D8 had a slightly lower R^2 of 0.982 but still showed precise predictions with a low MAE of 0.002. ND exhibited the highest RMSE of 0.024 and reasonable cross-validation performance with a CV error of 0.0065.

Densification notably impacts the flammability properties of wood, i.e., increase in the density reduces the porosity and limits oxygen penetration, thus enhancing its fire resistance [16]. The densification process enhanced the char formation during exposure to fire, i.e., the char layer insulates the underlying material, slowing down the heat transfer and reducing the combustion rate [9,11]. The insulating char layer acts as a thermal barrier, protecting the core of the wood and maintaining its structural integrity for an extended duration [1,9]. Moreover, past studies stated that densified wood has a lower heat release rate (HRR) than untreated ones [11]. The HRR is a key flammability parameter, as it measures the energy released during the combustion [6,8,10,23]. Lower HRR indicates that the densified wood releases energy more slowly, which reduces the fire intensity and makes it easier to control [16]. Besides that, the increased density of densified wood also improves its thermal stability, where it can withstand higher temperatures before igniting, thus improving fire resistance [3]. The enhanced thermal stability can be attributed to the compact structure of densified wood, which reduces the available surface area for fire propagation. A previous study reported that densified wood emits lower amount toxic smoke during combustion, attributed to its reduced porosity and compact structure [18]. In fact, lower smoke density and toxicity are essential for safe evacuation and reducing health risks associated with smoke inhalation, especially during fire outbreaks [1,5]. The enhanced fire resistance properties of densified wood provide additional safety and protection in buildings, contributing to the overall fire safety strategy [9,11].

4. Conclusions

This study showed that short-duration densification significantly enhanced the density and flammability properties of CLT. The densification process enhanced the laminas' density by up to 142.68%, with D8 achieving the highest improvement. The cone calorimeter test results indicated that increasing the compression ratio led to notable reductions in HRR and TSP, whereby D8 exhibited the lowest values, suggesting excellent fire resistance and smoke reduction properties.

The application of random forest models provided accurate and reliable predictions for both HRR and TSP, with the HRR model achieving metrics values that indicate strong predictive performance. Similarly, the model for TSP, using compression ratio, O2P, and CO2P as predictors, showed high accuracy and generalizability. In conclusion, this study suggests that densification can improve the flammability of CLT, and data-driven models such as random forest can be used to predict key flammability properties, thereby contributing to the development of safer and more durable timber structures.

Acknowledgement

The authors express thanks the Ministry of Higher Education (Malaysia), Universiti Malaysia Sabah, and the International Tropical Timber Organization (ITTO) for their funding support through the Fundamental Research Grant Scheme (FRGS/1/2022/TK10/UMS/02/1) and the ITTO Fellowship Programme (Reference No.: 070/21A).

References

- [1] Albert, Charles Michael, and Kang Chiang Liew. "Recent development and challenges in enhancing fire performance on wood and wood-based composites: A 10-year review from 2012 to 2021." *Journal of Bioresources and Bioproducts* 9, no. 1 (2024): 27-42. <https://doi.org/10.1016/j.jobab.2023.10.004>
- [2] Ayanleye, Samuel, Kenneth Udele, Vahid Nasir, Xuefeng Zhang, and Holger Militz. "Durability and protection of mass timber structures: A review." *Journal of Building Engineering* 46 (2022): 103731. <https://doi.org/10.1016/j.jobe.2021.103731>
- [3] Albert, Charles Michael, and Kang Chiang Liew. "Mass loss rate and charring rate of cross-laminated timber manufactured from densified low-density wood." In *AIP Conference Proceedings*, vol. 3110, no. 1. AIP Publishing, 2024. <https://doi.org/10.1063/5.0204712>
- [4] Younis, Adel, and Ambrose Dodoo. "Cross-laminated timber for building construction: A life-cycle-assessment overview." *Journal of Building Engineering* 52 (2022): 104482. <https://doi.org/10.1016/j.jobe.2022.104482>
- [5] Xu, Qingfeng, Yong Wang, Lingzhu Chen, Rundong Gao, and Xiangmin Li. "Comparative experimental study of fire-resistance ratings of timber assemblies with different fire protection measures." *Advances in Structural Engineering* 19, no. 3 (2016): 500-512. <https://doi.org/10.1177/1369433216630044>
- [6] Xu, Qingfeng, Lingzhu Chen, Kent A. Harries, Fuwen Zhang, Qiong Liu, and Jinghui Feng. "Combustion and charring properties of five common constructional wood species from cone calorimeter tests." *Construction and Building Materials* 96 (2015): 416-427. <https://doi.org/10.1016/j.conbuildmat.2015.08.062>
- [7] Nikolaeva, Marina, and Timo Kärki. "Influence of fire retardants on the reaction-to-fire properties of coextruded wood-polypropylene composites." *Fire and materials* 40, no. 4 (2016): 535-543. <https://doi.org/10.1002/fam.2308>
- [8] Le, Truong Di Ha, and Meng-Ting Tsai. "Experimental assessment of the fire resistance mechanisms of timber-steel composites." *Materials* 12, no. 23 (2019): 4003. <https://doi.org/10.3390/ma12234003>
- [9] Rinta-Paavola, Aleks, Dmitry Sukhomlinov, and Simo Hostikka. "Modelling Charring and Burning of Spruce and Pine Woods During Pyrolysis, Smoldering and Flaming." *Fire Technology* 59, no. 5 (2023): 2751-2786. <https://doi.org/10.1007/s10694-023-01458-9>
- [10] Ira, Jiří, Lucie Hasalová, Vojtěch Šálek, Milan Jahoda, and Václav Vystrčil. "Thermal analysis and cone calorimeter study of engineered wood with an emphasis on fire modelling." *Fire Technology* 56, no. 3 (2020): 1099-1132. <https://doi.org/10.1007/s10694-019-00922-9>
- [11] Wang, Zhengyang, Yuxin Gao, Yang Zhou, Chuangang Fan, Penghui Zhou, and Junhui Gong. "Pyrolysis and combustion behaviors of densified wood." *Proceedings of the Combustion Institute* 39, no. 3 (2023): 4175-4184. <https://doi.org/10.1016/j.proci.2022.08.057>
- [12] Zhao, Panpan, Chuigen Guo, and Liping Li. "Flame retardancy and thermal degradation properties of polypropylene/wood flour composite modified with aluminum hypophosphite/melamine cyanurate." *Journal of Thermal Analysis and Calorimetry* 135 (2019): 3085-3093. <https://doi.org/10.1007/s10973-018-7544-9>
- [13] Mantanis, George I., Jozef Martinka, Charalampos Lykidis, and Libor Ševčík. "Technological properties and fire performance of medium density fibreboard (MDF) treated with selected polyphosphate-based fire retardants." *Wood Material Science & Engineering* (2020). <https://doi.org/10.1080/17480272.2019.1596159>
- [14] Ma, Guoru, Xuan Wang, Wei Cai, Chao Ma, Xin Wang, Yulu Zhu, Yongchun Kan, Weiyi Xing, and Yuan Hu. "Preparation and study on nitrogen-and phosphorus-containing fire resistant coatings for wood by UV-cured methods." *Frontiers in Materials* 9 (2022): 851754. <https://doi.org/10.3389/fmats.2022.851754>
- [15] Hasburgh, L. E., and S. L. Zelinka. *Flammability and Acetic Acid Emissions from Acetylated Wood under Well-Ventilated Burning Conditions*. *Forests* 2023, 14, 1186. 2023. <https://doi.org/10.3390/f14061186>
- [16] Gan, Wentao, Chaoji Chen, Zhengyang Wang, Jianwei Song, Yudi Kuang, Shuaiming He, Ruiyu Mi, Peter B. Sunderland, and Liangbing Hu. "Dense, self-formed char layer enables a fire-retardant wood structural material." *Advanced Functional Materials* 29, no. 14 (2019): 1807444. <https://doi.org/10.1002/adfm.201807444>
- [17] Guo, Huizhang, Merve Özparpucu, Elisabeth Windeisen-Holzhauser, Christian M. Schlepütz, Elia Quadranti, Sabyasachi Gaan, Christopher Dreimol, and Ingo Burgert. "Struvite mineralized wood as sustainable building

- material: mechanical and combustion behavior." *ACS Sustainable Chemistry & Engineering* 8, no. 28 (2020): 10402-10412. <https://doi.org/10.1021/acssuschemeng.0c01769>
- [18] Chu, Demiao, Jun Mu, Stavros Avramidis, Sohrab Rahimi, Shengquan Liu, and Zongyuan Lai. "Functionalized surface layer on poplar wood fabricated by fire retardant and thermal densification. Part 1: Compression recovery and flammability." *Forests* 10, no. 11 (2019): 955. <https://doi.org/10.3390/f10110955>
- [19] Guo, Bingtuo, Yongzhuang Liu, Qi Zhang, Fengqiang Wang, Qingwen Wang, Yixing Liu, Jian Li, and Haipeng Yu. "Efficient flame-retardant and smoke-suppression properties of Mg–Al-layered double-hydroxide nanostructures on wood substrate." *ACS applied materials & interfaces* 9, no. 27 (2017): 23039-23047. <https://doi.org/10.1021/acsami.7b06803>
- [20] Schubert, M., M. Luković, and H. Christen. "Prediction of mechanical properties of wood fiber insulation boards as a function of machine and process parameters by random forest." *Wood Science and Technology* 54, no. 3 (2020): 703-713. <https://doi.org/10.1007/s00226-020-01184-3>
- [21] Jiang, Yanyan, Xiongqing Zhang, Jianguo Zhang, and Sophan Chhin. "Comparing the random forest algorithm with other modelling approaches to capture the complex patterns of intra-annual wood formation of Chinese fir with different ages." *Dendrochronologia* 77 (2023): 126043. <https://doi.org/10.1016/j.dendro.2022.126043>
- [22] ASTM, D. "2395-93. Standard Test Methods for Specific Gravity of Wood and Wood—Based Materials." *ASTM International: West Conshohocken, PA, USA* (2017). <https://doi.org/10.1520/D2395-14>
- [23] ISO, ISO. "5660-1: 2015 Reaction-to-fire tests-Heat release, smoke production and mass loss rate." *Heat Release Rate (Cone Calorimeter Method) and Smoke Production Rate (Dynamic Measurement)* (2015).
- [24] Angamuthu, Gokilavani, and P. Amudha. "Data-Driven Sales Forecasting for Fashion Sales using Machine Learning Techniques." *Journal of Advanced Research in Applied Sciences and Engineering Technology* (2024): 124-133. <https://doi.org/10.37934/araset.60.2.124133>
- [25] Müller, Katharina, Walter Sonderegger, Oliver Kläusler, Michael Klippel, and Edwin Zea Escamilla. "Mechanical characterisation of densified hardwood with regard to structural applications." *Journal of Renewable Materials* 8, no. 9 (2020): 1091-1109. <https://doi.org/10.32604/jrm.2020.09483>
- [26] Wang, Xianju, Dengyun Tu, Chuanfu Chen, Qiaofang Zhou, Huixian Huang, Zehao Zheng, and Zhipeng Zhu. "A thermal modification technique combining bulk densification and heat treatment for poplar wood with low moisture content." *Construction and Building Materials* 291 (2021): 123395. <https://doi.org/10.1016/j.conbuildmat.2021.123395>
- [27] Ma, Panpan, Xin An, Feibin Wang, Hui Huang, Zhiyuan Chen, Shuo Wang, Meng Gong, and Zeli Que. "Effects of pre-heating treatment parameters on dimensional stability and mechanical properties of densified Chinese fir." *Construction and Building Materials* 407 (2023): 133484. <https://doi.org/10.1016/j.conbuildmat.2023.133484>
- [28] Triquet, Juliette, Pierre Blanchet, and Véronique Landry. "Hardness of chemically densified Yellow birch in relation to wood density, polymer content and polymer properties." *Holzforschung* 75, no. 2 (2021): 114-125. <https://doi.org/10.1515/hf-2020-0076>
- [29] Srivaro, Suthon, Hyungsuk Lim, Minghao Li, Sataporn Jantawee, and Jaipet Tomad. "Effect of compression ratio and original wood density on pressing characteristics and physical and mechanical properties of thermally compressed coconut wood." *Construction and Building Materials* 299 (2021): 124272. <https://doi.org/10.1016/j.conbuildmat.2021.124272>
- [30] Cabral, John Paul, Bidur Kafle, Mahbube Subhani, Johannes Reiner, and Mahmud Ashraf. "Densification of timber: a review on the process, material properties, and application." *Journal of wood science* 68, no. 1 (2022): 20. <https://doi.org/10.1186/s10086-022-02028-3>
- [31] Bao, Minzhen, Xianai Huang, Mingliang Jiang, Wenji Yu, and Yanglun Yu. "Effect of thermo-hydro-mechanical densification on microstructure and properties of poplar wood (*Populus tomentosa*)." *Journal of Wood Science* 63 (2017): 591-605. <https://doi.org/10.1007/s10086-017-1661-0>
- [32] Kariz, Mirko, Manja Kitek Kuzman, Milan Sernek, Mark Hughes, Lauri Rautkari, Frederick A. Kamke, and Andreja Kutnar. "Influence of temperature of thermal treatment on surface densification of spruce." *European Journal of Wood and Wood Products* 75 (2017): 113-123. <https://doi.org/10.1007/s00107-016-1052-z>
- [33] Zhou, Qiaofang, Chuanfu Chen, Dengyun Tu, Zhipeng Zhu, and Kaifu Li. "Surface densification of poplar solid wood: effects of the process parameters on the density profile and hardness." *BioResources* 14, no. 2 (2019): 4814-4831. <https://doi.org/10.15376/biores.14.2.4814-4831>
- [34] Bekhta, Pavlo, Stanisław Proszkyk, Tomasz Krystofiak, Jan Sedliacik, Igor Novak, and Miroslava Mamonova. "Effects of short-term thermomechanical densification on the structure and properties of wood veneers." *Wood material science & engineering* 12, no. 1 (2017): 40-54. <https://doi.org/10.1080/17480272.2015.1009488>

- [35] Namari, Siavash, Lukas Drosky, Bianka Pudlitz, Peer Haller, Adeayo Sotayo, Daniel Bradley, Sameer Mehra et al. "Mechanical properties of compressed wood." *Construction and Building Materials* 301 (2021): 124269. <https://doi.org/10.1016/j.conbuildmat.2021.124269>